

# Active Power Filter for Variable-Speed Wind Turbine PMSG Interfaced to Grid and Non-linear Load via three Phase Matrix Converter

MOHAMED AMIN M.A. MOFTEH, EL-NOBY A. IBRAHIM & GABER EL-SAADY A. TAHA  
Electrical Engineering Department,  
Faculty of Engineering, Asyut University,  
Asyut  
EGYPT  
[Mhmoftah666@yahoo.com](mailto:Mhmoftah666@yahoo.com), [El-Saady@aun.edu.eg](mailto:El-Saady@aun.edu.eg)

*Abstract:* - the present paper aims to design an active power filter (APF) for harmonic mitigation of grid-connected wind turbine (WT). The wind energy conversion system (WECS) consists of permanent magnet synchronous generator (PMSG) driven by a variable-speed WT. The output of the PMSG is connected to a direct three phase AC/AC matrix converter (MC) to interface the system with the distribution grid. The MC controls the wind maximum power point tracking (MPPT) using perturbation and observation (P&O) method. The MC output current harmonics and non-linear load current harmonics are compensated by the proposed shunt (APF) based on d-q theory. The system under study is simulated using MATLAB/SIMULINK platform. The digital results show that, the proposed system is not only capable of delivering extracted wind power to the power system without currents/voltages harmonic distortion at grid side, but it can also satisfactorily eliminate harmonic currents which are drawn by non-linear load. The system dynamic performance is investigated under different wind speed and loading conditions. The system responses prove that the system works significantly irrespective of wind speed values and demanded load. Therefore the power quality in terms of grid current waveform, total harmonic distortion (THD) factor; frequency spectrum and system power factor is improved within permissible standard values as defined by IEEE-519.

*Key-Words:* - active power filter, grid connected system, harmonics mitigation, matrix converter, permanent magnet synchronous generator, power quality, and wind energy conversion system.

## 1 Introduction

The optimal usage of renewable energy sources (RES) will improve the overall performance of the electrical utility. RES and non-linear loads connected to grid have adverse effects on the power quality (PQ) of the system. Non-linear devices produce distorted current and voltage waveforms in the power system, due to the presence of power electronic switches in their structure, different harmonic components exist in the system, especially in the currents submitted/drawn to/from the utility grid. The injected harmonics have several impacts on the utilities grid and loads connected to system. To

overcome these PQ problems, harmonic active power filters (APF) are widely used in the system [1-6]. Using APF reduces system cost and also improves system reliability. Hence, the total harmonic distortion (THD) is kept as low as possible, improving the PQ of the power system.

## 2 Effect of Harmonics on the Wind Turbine Generators

Variable-speed wind turbine (WT) can be used in stand-alone mode or can be connected to the grid. A permanent magnet synchronous generator (PMSG) and double-fed induction generator (DFIG) are widely used because of their high performance and PQ features when compared with fixed speed WT. The majority of research interests related to grid-connected wind energy conversion system (WECS) due to the increasing ratio of installing WT with the grid in the last decade [7]. In this aspect, the control and operation of WT depend on active and reactive power control, fault ride through probability and compensation for non-linear and unbalanced loads. The typical characteristic of unbalanced load causing a non-linear current with high THD value, due to this non-linear current, the stator output voltage at point of common coupling (PCC) becomes non-sinusoidal with odd harmonic's (6n+1), multiples of fundamental frequency which deteriorates the performance of other connected loads with the generator [8]. Therefore, it is necessary to improve the PQ by eliminating these current harmonics, so to get pure sinusoidal output at PCC.

### 3 The Studied System Configuration

In this study, the analysis are focused on the system configuration with a direct coupling between shunt APF and the matrix converter (MC) of PMSG wind turbine as shown in Fig.1. Due to the random variation of wind velocities, maximum power point tracking (MPPT) technique based on perturbation and observation (P&O) algorithm is included in the speed control system of the PMSG, to make sure that WECS extracts the maximum power at all wind velocities. The MC controls the MPPT by adjusting the PMSG terminal frequency, and hence, the shaft speed. Also, the MC employed to inject the wind power into the utility grid (approximately at unity power factor) under various wind speed conditions. The space vector pulse width modulation (SV-PWM) is used to generate gating signals of MC switches.

### 4 Description of Wind Energy Conversion System

The WECS considered in this paper consists a PMSG driven by a variable speed WT. The output power from wind generator delivered to distribution grid through AC/AC matrix converter system. In this case study the total generated power flows through the converter.

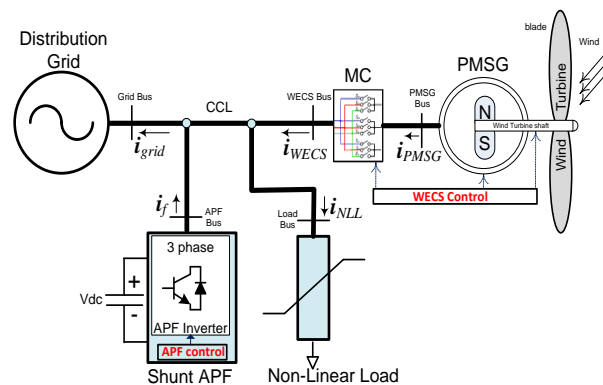


Fig.1 Basic schematic diagram of grid-tie variable speed direct-driven PMSG wind turbine linked to shunt APF and non-linear load

#### 4.1 Wind turbine background

In variable speed WT systems, the turbine is not directly connected to the utility grid. Instead, a power electronic interface is placed between the generator and the grid to provide decoupling and control of the system. Thus, the turbine is allowed to rotate at any speed over a wide range of wind speeds [9]. The wind kinetic energy is converted into mechanical power on the PMSG shaft through the WT. This PMSG converts the mechanical power into electrical power. The mechanical power can be formulated as follows:

$$P_{Mech} = 0.5 \rho C_p A V_w^3 \quad (1)$$

Where;  $P_{Mech}$  is the output mechanical power from WT in (W),  $\rho$  is the air density in ( $\text{kg/m}^3$ ),  $A$  is swept area of the turbine rotor in ( $\text{m}^2$ ), it equals ( $A=\pi R_r^2$ ) and  $R_r$  is the rotor blade radius in (m),  $C_p$  is WT power coefficient and  $V_w$  is the wind velocity in (m/s). The air density varies with air pressure and temperature, therefore  $\rho = 1.25 \text{ kg/m}^3$  for the purpose of this work, assuming that the air density  $\rho$  and the rotor area  $A$  are constant, the power coefficient  $C_p$  equals:

$$C_p = P_{mech} / P_{wind} \quad (2)$$

The power coefficient  $C_p$  is usually given as a function of the *tip speed ratio*  $\lambda$  and the *blade pitch angle*  $\theta$  as follows:

$$C_p = 0.5176 \left[ \frac{116}{\lambda_i} - (0.4\theta - 5) \right] \left[ \exp \left( \frac{-21}{\lambda_i} + 0.00086 \lambda \right) \right] \quad (3)$$

The pitch angle  $\theta$  is the angle between the plane of rotation and the blade cross section chord [9]; which

is considered zero in this case study, and  $\lambda_i$  defined by:

$$\lambda_i = \left( \frac{1}{\lambda + 0.08 \theta} - \frac{0.035}{\theta^3 + 1} \right)^{-1} \quad (4)$$

Therefore, the tip speed ratio  $\lambda$  of a WT is defined as:

$$\lambda = \frac{Tip_{speed}}{Wind_{speed}} = \frac{R_r \omega_m}{V_w} \quad (5)$$

Where  $R_r$  is the rotor radius in (m) and  $\omega_m$  is mechanical angular velocity of the generator (it equals WT rotor speed) in (rad/sec). There is an optimal value of the tip speed ratio  $\lambda$  which gives the maximum power coefficient  $C_p$  at which system operates at the MPP [10]. The relationship between power coefficient  $C_p$  and the tip speed ratio  $\lambda$  is usually provided by the WT manufacturer.

### 4.2 P&O Method for wind MPPT

MPPT is considered an essential part in the variable speed WT. Due to the random variation on the wind velocities, the electrical power generated from PMSG will vary also and unable to connect to the grid. P&O algorithm that is independent of the wind velocity detections has been used in this study. This method is based on perturbing the shaft generator speed in small step-size and observing the resulting changes in the output power until the slope becomes zero. The P&O method is a simple, robust and reliable technique and it presented in details in [11-13].

### 4.3 Matrix Converter as a Power Conditioning System

Since the variable speed rotor of the WT is directly coupled to the PMSG, this later produces an output voltage with variable amplitude and frequency. This condition demands the use of an extra conditioner to meet the amplitude and frequency requirements of the utility grid. The AC/AC matrix converter is applied in this study. It is a single-stage AC/AC bi-directional power flow converter that takes power from AC source and converts it to another AC system with different amplitude and frequency. It has the ability to control the output voltage magnitude and frequency in addition to operation at approximately unity power factor in order to inject only active power to the grid. It can also control the PMSG speed in order to track the MPP at all wind

speed values based on P&O technique. Moreover, it provides approximately sinusoidal input and output waveforms, with minimal higher order harmonics and no sub-harmonics. The complete structure and switching scheme of MC was presented in [14-20].

## 5 Proposed Control Algorithm of WECS

The structure of the proposed control algorithm of WECS is outlined in Fig.2. The WT generation system takes wind speed  $V_w$  and PMSG angular speed  $\omega_m$  as inputs. The developed output torque  $T_m$  of the WT is applied to the PMSG shaft as a mechanical input torque. The direction of the torque  $T_m$  is positive during motoring mode of the machine and made negative during generating mode of PMSG.

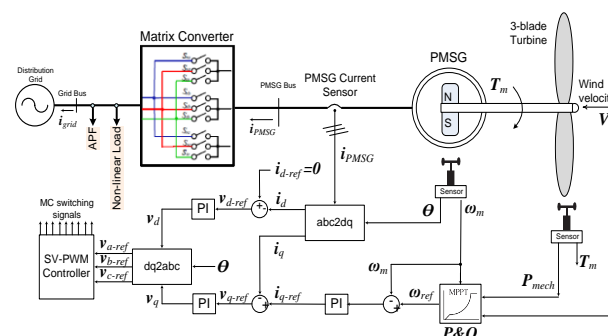


Fig.2. Block diagram of the WECS control algorithm

The P&O block takes the PMSG rotor speed  $\omega_m$  and WT mechanical power  $P_{mech}$  as input to provide the estimated value of the MPP speed  $\omega_{ref}$  that achieves MPP extracted at this wind velocity  $V_w$ . The reference generator speed  $\omega_{ref}$  is compared with the actual generator speed  $\omega_m$  and the error signal is applied to conventional PI controllers to generate the reference value for the q-axis component  $i_{q\_ref}$ ; on the other hand the reference value for the d-axis component  $i_{d\_ref} = 0$  in order to keep the d-axis component flux equals zero.

The actual three phase stator current signals of the generator  $i_{PMSG}$  are measured and converted to the  $d-q$  axis component  $i_{d-iq}$  using Park/Clark Transformation. The actual currents in the  $d-q$  axis components  $i_{d-iq}$  are compared with their reference values ( $i_{d\_ref} - i_{q\_ref}$ ) and the error signal is applied to conventional PI controllers to generate the reference  $d-q$  axis voltage components ( $v_{d\_ref} - v_{q\_ref}$ ). The gains of the PI controllers have been manually tuned in order to achieve acceptable transient response. The  $d-q$  reference voltage components ( $v_{d\_ref} - v_{q\_ref}$ ) are converted to the

three-phase axis using the invers Park/Clark transformation in order to obtain the three-phase reference voltage ( $v_{a\_ref}$ ,  $v_{b\_ref}$ ,  $v_{c\_ref}$ ). The three-phase reference voltages are used in the MC controller to generate switching pulses of the MC. The SV-PWM control technique with 6 kHz of switching frequency is used for this purpose. It is better than conventional PWM techniques because of its advantages as it generates controlled output voltage magnitude and frequency, it generates lower THD and it is suitable for digital controllers [21]. Fig.3 presents the details of the grid-tie WECS including PMSG, the MC and its control circuit and the LC input filter. The PMSG has 4 pairs of poles ( $P=4$ ), its stator resistance & inductance are ( $R_{sator}=2.875 \Omega$ ,  $L_d = L_q=8.5 \text{ mH}$ ), the PMSG moment of inertia ( $J=0.00008 \text{ kg.m}^2$ ) and the PMSG flux linkage ( $\Psi=0.175 \text{ wb}$ ).

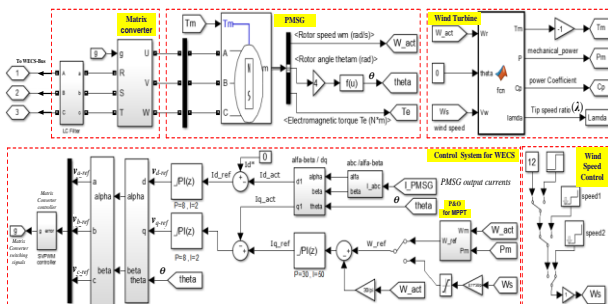


Fig.3. MATLAB/SIMULINK model of WT system based on PMSG and three-phase matrix converter

## 6 Basic Compensation Principle of Shunt APF

The basic compensation principle of the APF is to detect the unwanted harmonic components of the line currents and then to generate and inject a signal into the line in such a way to produce partial or total cancellation of the unwanted components. The proposed shunt APF is controlled using instantaneous active and reactive current component  $i_d$ - $i_q$  method [22] which provides efficient way to get rid of the harmonics resulted from the WECS and non-linear load. Such the control of the APF is achieved through the line current  $i_L$ , filter current  $i_f$ , and the DC voltage  $V_{dc}$  as shown in Fig.4 Each component of the proposed control system will be explained in the following subsections.

### 6.1 The Shunt APF Structure

The APF is shunt connected at common coupling line (CCL) between WECS and the distribution grid. The APF design criteria as shown in Fig.4 compose; a current controlled voltage source inverter (CC-

VSI) power circuit, smoothing inductor  $L_f$ , DC capacitor  $C_{dc}$  and the APF control circuit to obtain the reference currents. The VSI contains three phase Isolated Gate Bipolar transistor (IGBT) with anti-parallel diodes connected to the DC capacitor located at the DC bus of the IGBT, to serve as an energy storage element for providing a constant DC voltage for real power necessary to cover the APF losses at steady state.

### 6.2 Current supplied by the shunt APF

From Fig.4 it is seen that; the APF is controlled to draw/supply a filter compensating current  $i_f$  from/to the system, so that it cancels current harmonics at the CCL, hence it improves the submitted current to utility grid to be pure sinusoidal and at the same time it makes current and voltage at grid side in phase without harmonic distortion. The filter compensating current  $i_f$  injected by APF contains all harmonics, to make current at grid side pure sinusoidal. The detailed equations which describe the shunt APF concept were presented in [23].

## 7 APF Control Method

The quality and performance of the shunt APF is based on control circuit to generate the reference currents, that must be provided by the filter to compensate line reactive power and harmonic currents. This involves a set of currents in the phase domain, which will be tracked generating the switching signals applied to VSI by means of the hysteresis control switching technique, such that the desired current reference is exactly followed.

### 7.1 Compensating Reference Currents

The control strategy for a shunt APF configuration requiring measurement of both actual line currents and filter currents. The actual filter currents are compared with reference currents as shown in Fig.4. The comparison results is fed to gate pulse generation system with hysteresis band (HB) control. The HB current regulators have been widely used for APF applications because of their high bandwidth, simple structure and it is the fastest control with minimum hardware and software [24]. As illustrated in Fig.4, The distorted measured line currents ( $i_{La}$ ,  $i_{Lb}$ ,  $i_{Lc}$ ) are transferred into synchronous rotating frame ( $i_{Ld}$ ,  $i_{Lq}$ ) using  $abc$  to  $dq0$  transformation block [22] using the phase locked loop (PLL) circuit to maintain the synchronization with supply system.



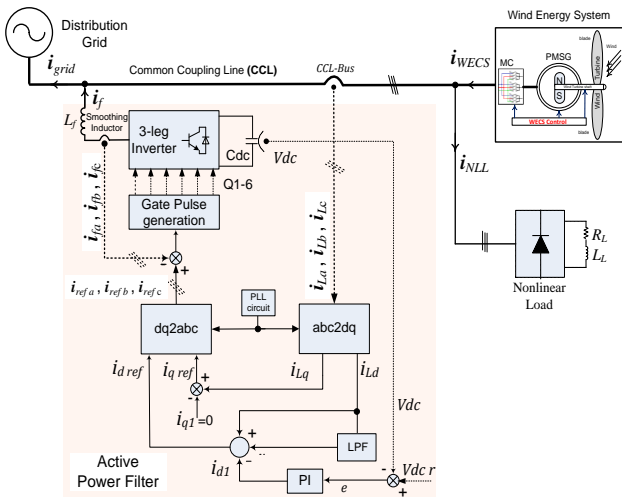


Fig. 4. The shunt APF system configuration & its control circuit

Using a low pass filter (LPF) and compensation current control, the ac active current harmonics components of line current ( $i_{d-ref}$ ) are derived. The reactive power flow is controlled by the fundamental harmonic quadrature current  $i_{Lq}$ . However, considering the primary end of the APF is simply to eliminate current harmonics, the current  $i_{q1}$  is set to zero as shown in Fig. 4. The harmonic reference currents ( $i_{d-ref}$ ,  $i_{q-ref}$ ) are transformed to ( $i_{ref-a}$ ,  $i_{ref-b}$ ,  $i_{ref-c}$ ) through  $dq0$  to  $abc$  transformation block.

**7.2 DC Voltage Regulation**

The DC bus proportional integral PI controller as shown in Fig.4, regulates the DC bus voltage  $V_{dc}$  to its reference value  $V_{dcr} = 400v$ , and compensates for the inverter losses. The DC capacitor voltage is sensed and then compared with a reference value. The obtained error ( $e = V_{dcr} - V_{dc}$ ) used as input for PI controller, the DC bus controller generates a fundamental harmonic direct current  $i_{q1}$  to provide the active power transfer required to regulate DC bus voltage and compensate the inverter losses.

**7.3 The gate pulse generation system**

The proposed shunt APF uses a fixed HB controller to compensate for the unwanted line currents. It derives the switching signals of the CC-VSI from the current error. Where the harmonic reference currents ( $i_{ref-a}$ ,  $i_{ref-b}$ ,  $i_{ref-c}$ ) are compared to the actual filter currents ( $i_{f-a}$ ,  $i_{f-b}$ ,  $i_{f-c}$ ) and produce the error which is the input to the HB current controller to keep the current within the HB and to produce gate

switching control pulses (Q1-Q6) for the IGBTs bridge.

**8 Simulation Results and Discussion**

The proposed grid-tie WECS based on PMSG linked to shunt APF and non-linear load through direct matrix converter system is not only capable of supplying extracted wind power to the utility grid without currents/voltages harmonic distortion, but it can also significantly mitigate harmonic currents which are caused by both non-linear load and power electronics in AC/AC matrix conversion stage. In order to demonstrate the validity of the concept discussed previously a simulation using MATLAB/SIMULINK environment is done as indicated in Fig.5. The system model consists of four blocks, WT generation block, distribution utility grid block, non-linear load block and the APF block. These blocks are connected together at CCL through low voltage cables. The grid line voltage is 200v with 50Hz frequency and the whole system parameters values used in the simulation are shown in Fig.5.

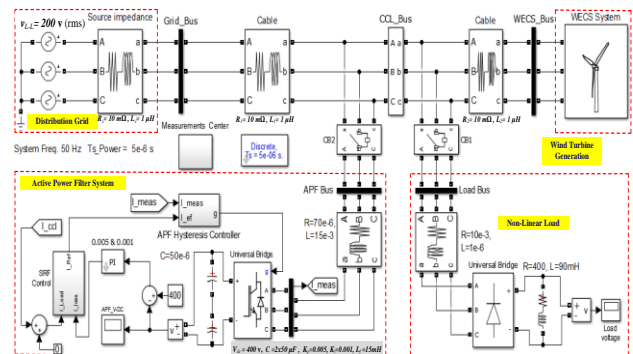


Fig.5 The complete MATLAB/SIMULINK model of wind renewable energy source tied to distribution grid with APF and non-linear load

Fig.6 describes the wind speed profile applied in this study which vary from (8-12-10 m/s) at time periods of (0-0.2-0.4 sec) respectively. During the simulation, the values of power coefficient  $C_p$  and tip speed ratio  $\lambda$  of the WT are remain constant at their optimal values ( $C_p = 0.48$  and  $\lambda = 8.1$ ) to give MPP regardless of the variation in wind speed.

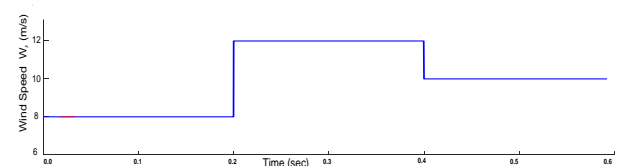


Fig.6 Wind speed profile

Two simulation *scenarios* have been performed to evaluate the performance of the proposed shunt APF on the grid currents under variable wind speed conditions. During the two scenarios, the shunt APF is (in OFF state) during periods (0.0-0.1s, 0.2-0.3s & 0.4-0.5s). While it is commanded to be active (in ON state) during periods (0.1-0.2s, 0.3-0.4s & 0.5-0.6s), to compensate the harmonics in grid currents. The phase “a” waveforms and their associated Fast Fourier Transform (FFT) analysis are only illustrated in the next figures.

### 8.1 Scenario#1 (The standalone shunt APF with WECS)

To evaluate the influence of the standalone shunt APF on WECS, the non-linear load is deactivated to be out of service during this scenario. Fig.7.a represents the grid voltage and grid current waveforms and Fig.7.b shows the injected filter current waveform for phase “a”, for different wind speed conditions (8, 12 & 10 m/s).

The same grid currents are represented on Fig.8.a, Fig.8.b and Fig.8.c. in line with their associated FFT analysis. Fig.7.a shows the grid phase voltage and its corresponding grid line current. It is clear that the grid current and grid voltage are out of phase by 180 degree. This phase shift indicates that the power is delivered to utility grid not received. Therefore, the wind turbine injects active power only to the utility grid with unity power factor.

From Fig.7.a, we can observe the influence of the wind speed, and therefore the kinetic energy of wind on the amplitudes of grid current in the period between (0.2-0.4s). With the increase of the wind speed, currents values become more in the grid side.

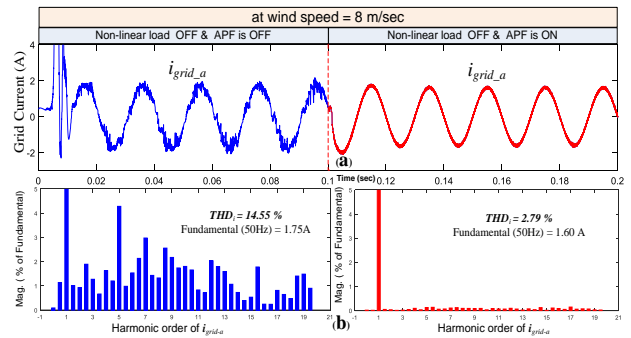


Fig.8 (a) WECS grid current waveform ( $i_{grid\_a}$ ) & its FFT analysis, without non-linear load at wind speed=8 m/s

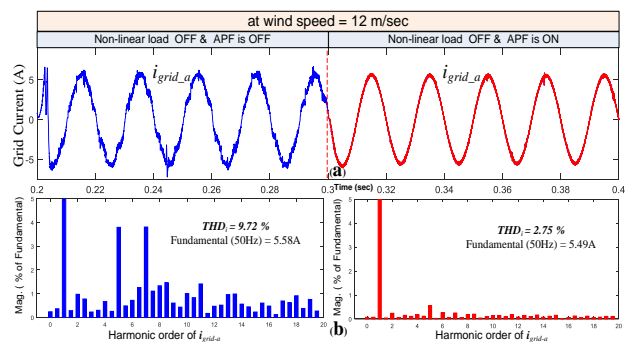


Fig.8 (b) WECS grid current waveform ( $i_{grid\_a}$ ) & its FFT analysis, without non-linear load at wind speed=12 m/s

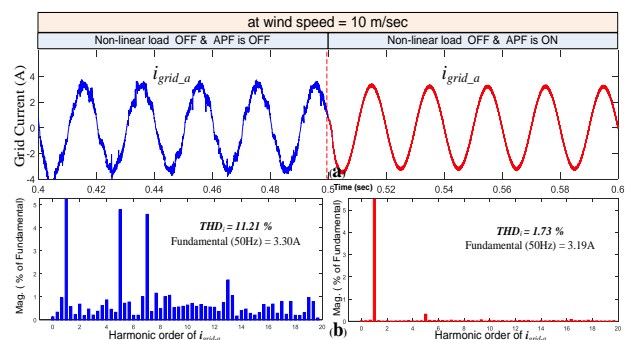


Fig.8 (c) WECS grid current waveform ( $i_{grid\_a}$ ) & its FFT analysis, without non-linear load at wind speed=10 m/s

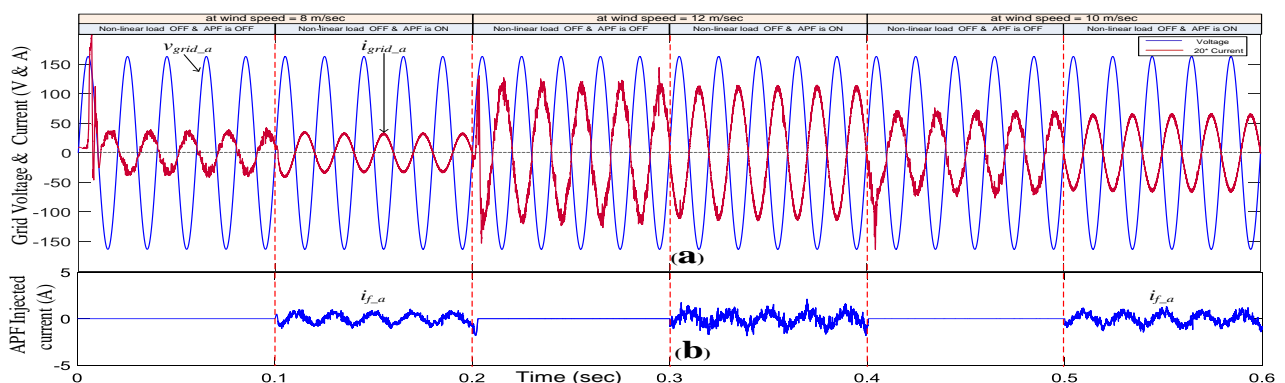


Fig.7 (a) Grid voltage & current ( $v_{grid\_a}$  &  $i_{grid\_a}$ ) (b) Injected filter current ( $i_{f\_a}$ ) - without non-linear load at different wind speed conditions

The upper parts of Fig.8.a, Fig.8.b & Fig.8.c show the WECS currents which submitted to the distribution utility grid without and with active filtering. The lower parts of the same figures provide the FFT analysis of the submitted current to the utility grid. We can observe after connecting the shunt APF at (t = 0.1 s, 0.3 s & 0.5s) and during active filter operating time, the grid current waveform approaches more than sinusoidal form, and harmonic currents are compensated to standard values as summarized in Table 1.

At wind speed	% THD		% THD reduction Improvement
	APF is ON	APF is OFF	
8 m/s	14.55	2.79	80.82
12 m/s	9.72	2.75	71.70
10 m/s	11.21	1.73	84.57

**8.2 Scenario#2 (The APF with WTG system in the presence of non-linear load)**

In this scenario, the non-linear load is connected to CCL to be in service (in ON state). Fig.9.a represents the grid voltage and current waveforms, Fig.9.b shows the injected filter current & Fig.9.c shows the non-linear load current waveform for phase “a”, for different wind speed conditions (8, 12 & 10 m/s). The same grid currents and their associated FFT analysis are represented on the Figs.10.a, 10.b and 10.c.

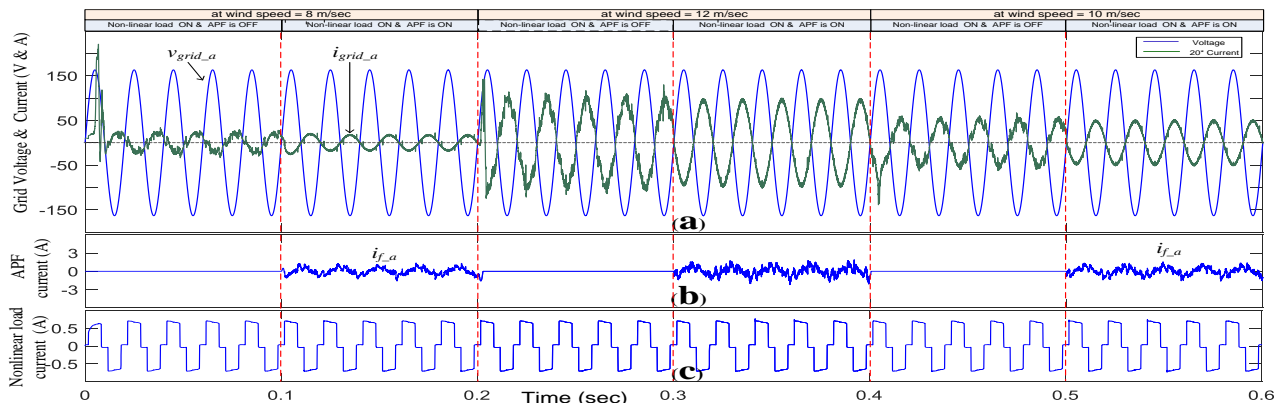


Fig.9 (a) Grid voltage & current  $v_{grid\_a}$  &  $i_{grid\_a}$  (b) Injected filter current  $i_{f\_a}$  (c) Non-linear Load current  $i_{NLL\_a}$  at different wind speed conditions

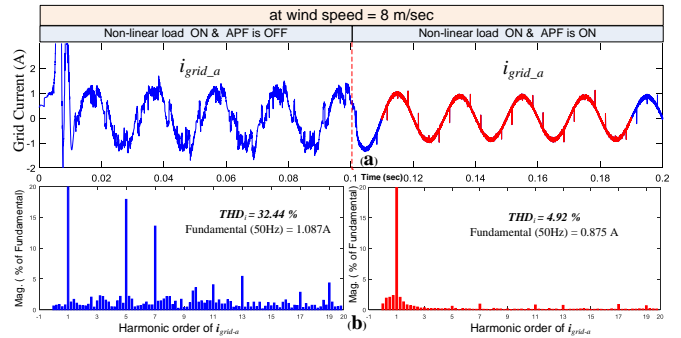


Fig.10 (a) WECS grid current waveform ( $i_{grid\_a}$ ) & its FFT analysis, in the presence of non-linear load, at wind speed=8 m/s

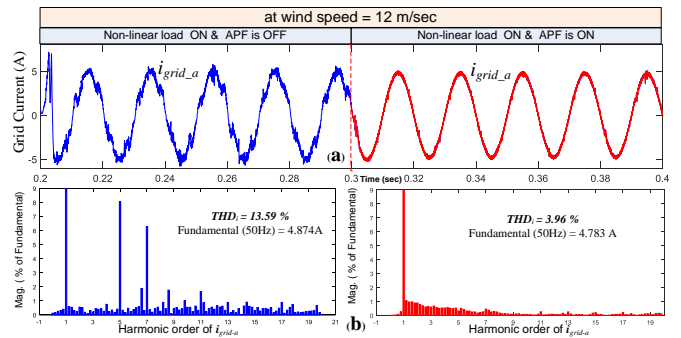


Fig.10 (b) WECS grid current waveform ( $i_{grid\_a}$ ) & its FFT analysis, in the presence of non-linear load, at wind speed=12 m/s

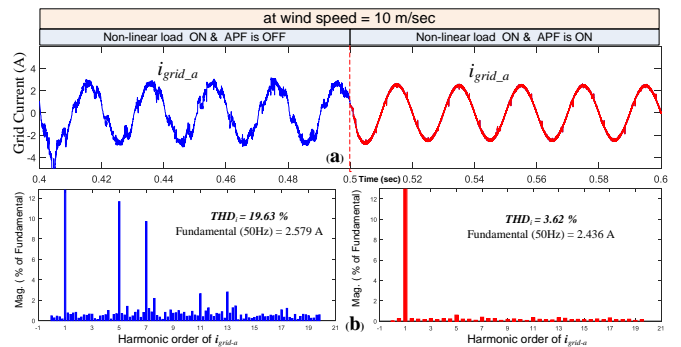


Fig.10 (c) WECS grid current waveform ( $i_{grid\_a}$ ) & its FFT analysis, in the presence of non-linear load, at wind speed=10 m/s

Fig.9.a shows the effectiveness of the AC/AC matrix converter for providing the active power only to the utility grid with unity power factor whether the APF is in service or out of service.

The upper parts of Fig.10.a, Fig.10.b & Fig.10.c show the delivered WECS currents to the distribution grid in the presence of non-linear load, without and with active filtering. We can observe after connecting APF at (t = 0.1 s, 0.3 s & 0.5s) and during active filter operating time, the grid current waveform becomes more sinusoidal. The lower parts of the same figures provide the FFT analysis of the submitted current to the grid, which show a decrease in the THD of the grid current waveform to good level within acceptable standard values as indicated in Table 2.

<b>Table 2</b>			
% THD of the WECS submitted current to distribution grid before and after compensation in the presence of non-linear load			
At wind speed	% THD		% THD reduction Improvement
	APF is ON	APF is OFF	
8 m/s	32.44	4.92	84.30
12 m/s	13.59	3.96	70.86
10 m/s	19.63	3.62	81.55

## 9 Conclusion

The performance and feasibility of the proposed grid-tie WECS based on PMSG interfaced to shunt APF and non-linear load through direct matrix converter was realized and verified through simulation studies using MATLAB /SIMULINK under different operating conditions. The connection of the WECS to the grid takes place in one stage using the direct AC/AC matrix converter. Meanwhile, the methodology of dynamic shunt APF with its adaptive control was used to enhance PQ at utility end in a grid system connected to wind renewable energy source. The APF design, structure and its control system was also presented. The simulated system is subjected to nonlinear load disturbances to study the effectiveness of the proposed shunt APF. The shunt APF allows the harmonics present in the utility system to be compensated, providing a good PQ of supply to customers. The digital results prove that the proposed APF is not only capable of delivering the

wind power to the distribution grid with acceptable THD, but will also act to mitigate the current harmonics injected by the non-linear loads.

The obtained results demonstrate that the shunt APF performs very well in spite of variation in wind speed. Also, maximum power extraction from WT can be achieved through SV-PWM control technique at the generator side to generate switching signals of AC/AC matrix converter. The MPPT algorithm based on P&O method is included. Simulation results prove that, in the presence of the shunt APF, the wind turbine system tracks the MPP and injects only pure sinusoidal active currents to the distribution grid at all wind speeds, whether there is non-linear load or without non-linear load.

Furthermore the simulation shows that the proposed shunt APF offers better sinusoidal grid current waveform with approximately 80% improvement of THD reduction as illustrated in tables 1&2.

### References:

- [1] Pallagiri Venkata Dinesh Reddy, S. Chandra mouli, "Hybrid Renewable Energy Sources Based Four Leg Inverter for Power Quality Improvement", International Journal of Advanced Technology and Innovative Research, Volume.07, No.06, pp.1092-1098, July-2015.
- [2] Sudheer Kasa, P. Ramanathan, S.amasamy , D.P. Kothari; " Effective grid interfaced renewable sources with power quality improvement using dynamic active power filter", Proceedings of Electrical Power and Energy Systems 82, pp.150–160, 2016.
- [3] Senthilkumar. A ,Poongothai. K, Selvakumar. S, Silambarasan. Md, P. Ajay-D-VimalRaj "Mitigation of Harmonic Distortion in Microgrid System using Adaptive Neural Learning Algorithm based Shunt Active Power Filter " SMART GRID Technologies, Procedia Technology 21, PP.147-154, August 2015.
- [4] H. H. Tumbelaka, Lawrence J. Borle, Chemmangot V. Nayar and Seong Ryong Lee, "A Grid Current Controlling Shunt Active Power Filter", Journal of Power Electronics, Vol. 9, No. 3, May 2009.
- [5] Sajid Hussain Qazi, Mohd Wazir Mustafa, "Review on active filters and its performance with grid connected fixed and variable speed wind turbine generator" Renewable and Sustainable Energy Reviews, Science Direct 57, pp. 420–438, 2016.
- [6] H. H. Tumbelaka, C. V. Nayar, K. Tan, and L. J. Borle, "Active filtering applied to a line-



- commutated inverter fed permanent magnet wind generator*", International Power Engineering Conference IPEC2003, Singapore, 2003.
- [7] Oğuz Y, Güney İ, Çalık H. "Power quality control and design of power converter for variable-speed wind energy conversion system with permanent-magnet synchronous generator". *Sci-World-July*; 2013:1–14, 2013.
- [8] Phan V-T, Lee H-H. "Control strategy for harmonic elimination in stand-alone DFIG applications with nonlinear loads". *IEEE Trans. Power Electron*; 26: 2662–75, 2013.
- [9] E. Hau, "Wind Turbines: Fundamentals, Technologies, Application, Economics", 2nd edition. Berlin, Germany: Springer, 2006.
- [10] Q. Wang and L. Chang, "An intelligent maximum power extraction algorithm for inverter-based variable speed wind turbine systems," *Power Electronics, IEEE Transactions on*, vol. 19, pp. 1242-1249, 2004.
- [11] M. Abdullah, A. Yatim, C. Tan, and R. Saidur, "A review of maximum power point tracking algorithms for wind energy systems," *Renewable and Sustainable Energy Reviews*, vol. 16, pp. 3220-3227, 2012.
- [12] A. Mahdi, W. Tang, and Q. Wu, "Estimation of tip speed ratio using an adaptive perturbation and observation method for wind turbine generator systems," in *Renewable Power Generation (RPG 2011)*, IET Conference on, pp. 1-6, 2011.
- [13] J. S. Thongam and M. Ouhrouche, "MPPT control methods in wind energy conversion systems," *Fundamental and Advanced Topics in Wind Power*, pp. 339-360, 2011.
- [14] D. Casadei, G. Grandi, G. Serra, and A. Tani, "Space vector control of matrix converters with unity input power factor and sinusoidal input/output waveforms," in *Power Electronics and Applications, 1993.*, Fifth European Conference on, pp. 170-175, 1993.
- [15] P. W. Wheeler, J. Rodriguez, J. C. Clare, L. Empringham, and A. Weinstein, "Matrix converters: a technology review," *Industrial Electronics, IEEE Transactions on*, vol. 49, pp. 276-288, 2002.
- [16] A. Alesina and M. Venturini, "Solid-state power conversion: A Fourier analysis approach to generalized transformer synthesis," *Circuits and Systems, IEEE Transactions on*, vol. 28, pp. 319-330, 1981.
- [17] A. Alesina and M. Venturini, "Analysis and design of optimum-amplitude nine-switch direct AC-AC converters," *Power Electronics, IEEE Transactions on*, vol. 4, pp. 101-112, 1989.
- [18] J. Rodriguez, M. Rivera, J. W. Kolar, and P. W. Wheeler, "A review of control and modulation methods for matrix converters," *IEEE Transactions on Industrial Electronics*, vol. 59, pp. 58-70, 2012.
- [19] J. Rodriguez, E. Silva\*, F. Blaabjerg, P. Wheeler, J. Clare, and J. Pontt, "Matrix converter controlled with the direct transfer function approach: analysis, modelling and simulation," *International journal of electronics*, vol. 92, pp. 63-85, 2005.
- [20] L. Zhang, C. Watthanasarn, and W. Shepherd, "Control of AC-AC matrix converters for unbalanced and/or distorted supply voltage," in *Power Electronics Specialists Conference, 2001. PESC. 2001 IEEE 32nd Annual*, pp. 1108-1113, 2001.
- [21] M. Y. Lee, P. Wheeler, and C. Klumpner, "Space-vector modulated multilevel matrix converter," *Industrial Electronics, IEEE Transactions on*, vol. 57, pp. 3385-3394, 2010.
- [22] R. S. Herrera and P. Salmerón, "Instantaneous Reactive Power Theory: A Reference in the Nonlinear Loads Compensation", *IEEE Transactions on Industrial Electronics*, Vol. 56, No. 6, pp. 2015-2022, June 2009.
- [23] A. Eid, M. Abdel-Salam, H. El-Kishky, T. El-Mohandes, "Active power filters for harmonic cancellation in conventional and advanced aircraft electric power systems", "Electric Power Systems Research", 2008.
- [24] D. -H. Chen and S. -J. Xie, "Review of Control Strategies Applied to Active Power Filters," *Proceedings of the IEEE International Conference on Electric Utility Deregulation, Restructuring and Power Technologies (DRPT)*, Hong Kong, pp. 666-670, 2004.